Appl. Phys. B 86, 71–75 (2007)
DOI: 10.1007/s00340-006-2370-3

Applied Physics B
Lasers and Optics

Z. ZHU[1]
J. LI[1]
B. ALAIN[2]
G. JIA[1]
Z. YOU[1]
X. LU[1]
B. WU[1]
C. TU[1,✉]

Growth, spectroscopic and laser properties of Yb^{3+}-doped $GdAl_3(BO_3)_4$ crystal: a candidate for infrared laser crystal

[1] Fujian Institute of Research on the Structure of Matter, Chinese Academy of Sciences, Fuzhou, Fujian, 350002, P.R. China
[2] Laboratoire de Physico-Chimie des Matériaux Luminescents, UMR CNRS 5620, Université Claude Bernard-Lyon1, 69622 Villeurbanne, France

Received: 14 April 2006/Revised version: 30 May 2006
Published online: 11 July 2006 •

ABSTRACT Yb^{3+}:$GdAl_3(BO_3)_4$ (hereafter Yb^{3+}:GAB) crystals with large sizes and good optical quality have been grown by the top-seed solution growth (TSSG) method. The polarized absorption and emission spectra have been investigated at room temperature. For the σ-polarization, the intensities of both absorption and emission spectra are stronger than those for the π-polarization, the σ-absorption cross section of Yb^{3+} in GAB being 3.43×10^{-20} cm^2 at 977 nm, and the σ-emission cross section being 0.98×10^{-20} cm^2 at 1045 nm. The fluorescence lifetime of the $^2F_{5/2} \to {}^2F_{7/2}$ transition was measured to be 800 μs in the 5% doped sample used for our laser experiments, 993 μs in a 10% doped sample and 569 μs in a 0.5% doped sample. The laser parameters were estimated as: $\beta_{min} = 0.022$, $I_{sat} = 10.4$ kW/cm^2 and $I_{min} = 0.23$ kW/cm^2. About 0.4 W laser output at the wavelength of 1043 nm was achieved when the Yb^{3+}:GAB crystal was pumped by a 974 nm laser diode, with 27.4% slope efficiency.

PACS 42.55.-f; 42.70.Hj; 78.20.-e; 81.10.Dn

1 Introduction

During the last decade, Yb^{3+}-doped materials have attracted an increasing interest for their potential application in high efficiency solid-state laser systems with the development of high-power diode sources [1–3], due to the Yb^{3+} ion's advantages over other trivalent rare earth ions. The Yb^{3+} ion has a $4f^{13}$ shell, which lacks one electron compared with a full filled shell. There are only two energy levels, the ground state $^2F_{7/2}$ and the excited state $^2F_{5/2}$, which are separated by approximately 10 000 cm^{-1}. As a result, in Yb^{3+}-doped laser materials, some detrimental phenomena affecting laser performance are absent, such as excited state absorption and up-conversion, which normally exist in Nd^{3+} and Er^{3+}-doped laser media, or are moderated such as luminescence concentration quenching. Moreover, the Yb^{3+} ion presents a long radiative lifetime value and high quantum efficiency, so that the pump induced heating of the crystal during laser operation is efficiently reduced. Thus, the spectroscopic and laser performance of Yb^{3+}-doped materials have been widely investigated, for example, Yb^{3+}:YAG [1, 2], Yb^{3+}:FAP [4, 5], Yb^{3+}:YAB [6], Yb^{3+}:YCOB [7], and Yb^{3+}:GCOB [8].

The $GdAl_3(BO_3)_4$ crystal belongs to a trigonal system with the space group $R32$. The GAB crystal has been demonstrated to be a good host material for solid-state lasers because of its good chemical and physical properties, such as high chemical stability and mechanical strength. Due to its nonlinear optical coefficients, GAB crystal doped with Nd^{3+} ions, is a host for lasers, emitting at wavelengths in the infrared, red, green, blue and ultraviolet regions by self-frequency conversions [9–11]. In addition, near infrared, yellow and green lasers have been achieved through Yb^{3+}:YAB crystal [12], which has the same structure and nonlinear optical properties as GAB crystal. In this paper, we report the growth, spectroscopic and laser properties of Yb^{3+}:$GdAl_3(BO_3)_4$ crystal.

2 Crystal growth

The crystal growth was carried out in a vertical tubular muffle furnace controlled by an AI-808P artificial intelligence industrial controller to ensure the maintenance of temperature with an accuracy of ±0.2 °C and a programmed cooling rate. A Pt crucible of 60 mm diameter by 60 mm high was used.

The crystal was grown using $K_2Mo_3O_{10}$-B_2O_3 as the flux. The mixtures were synthesized according to the following reactions:

$$x Yb_2O_3 + (1-x) Gd_2O_3 + 3Al_2O_3 + 8H_3BO_3 \to 2Yb_xGd_{1-x}Al_3(BO_3)_4 + 12H_2O \uparrow$$

$$3MoO_3 + K_2CO_3 \to K_2Mo_3O_{10} + CO_2 \uparrow$$

$$2H_3BO_3 \to B_2O_3 + 3H_2O \uparrow$$

where $x = 0.005, 0.05$ and 0.10 are the doping concentrations. The raw chemicals used were Al_2O_3, H_3BO_3, K_2CO_3, MoO_3 (analytical grade) and Gd_2O_3, Yb_2O_3 (99.99%). The starting materials of 20 wt. % Yb^{3+}:GAB, 72 wt. % $K_2Mo_3O_{10}$ and 8 wt. % B_2O_3 were thoroughly mixed and slowly heated to 1100 °C, and kept at this temperature for 2 days to homogenize the solution. By seeding several times, the saturation temperature was determined exactly to be 1021 °C, and the

✉ Fax: +86-591-83714946, E-mail: tcy@fjirsm.ac.cn

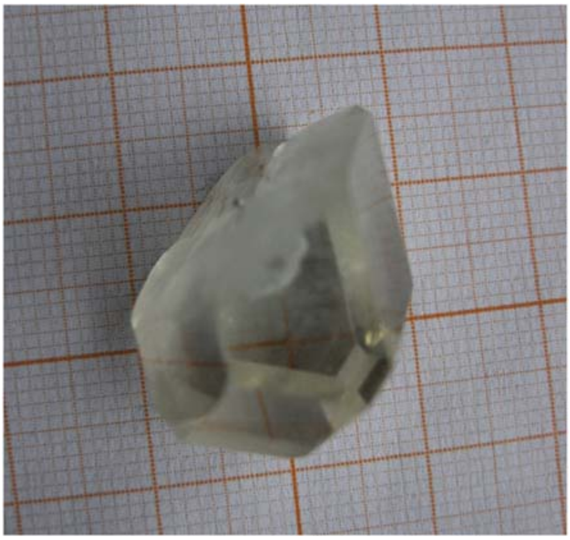

FIGURE 1 The as-grown crystal of Yb^{3+}:GAB

c-axis crystal seed with the size of $8 \times 3 \times 3\,mm^3$ was immersed into the solution. The growing crystal was rotated at a rate of 10–25 rpm, and the cooling rate was 1–3 °C/day. After about 40 days, the process was over and the crystal was drawn out of the melt. Then it was cooled down to room temperature at the rate of 50 °C/h.

The as-grown crystal of Yb^{3+}:GAB is shown in Fig. 1. The concentration of Yb^{3+} ions in Yb^{3+}:GAB doped with 5% was measured to be 1.18 wt. % by means of the ICP-AES method, thus the Yb^{3+} ion concentration in this crystal was $1.80 \times 10^{20}\,cm^{-3}$. Thus the segregation coefficient of Yb^{3+} ions in this crystal is 0.65.

3 Spectroscopy analysis

A sample of 5% doped crystal cut along the c crystallographic axis with a thickness of 2.0 mm was subjected to spectroscopic experimentation. The σ- ($E \perp c$) and π- ($E \parallel c$) polarized absorption spectra of the Yb^{3+}:GAB crystal were recorded by a Perkin-Elmer UV-VIS-NIR spectrophotometer (Lambda900) at room temperature. The polarized luminescence spectra and the fluorescence decay curves excited by 980 nm light were measured at room temperature using an Edinburgh Analytical Instruments Fluorescence Spectrometer (FLS920), with a xenon lamp light source. Because of the weak pump light reflection and scatter due to the good crystal quality, the fluorescence could be detected near 980 nm at the same wavelength as the pump. The decays were also measured by pumping with a nano-second optical parametric oscillator from BM Industries emitting near 980 nm and a digital Lecroy oscilloscope.

The polarized absorption spectra of Yb^{3+}:GAB crystal are shown in Fig. 2. It can be easily shown that the σ-polarized absorption is much stronger than the π-polarized one. In the σ-polarized absorption spectrum, there are two main absorption peaks, which are centered at 977 nm and 935 nm, respectively. The absorption peak at the wavelength of 977 nm is the strongest one in the measured range, which matches very well with the emitting wavelength of InGaAs laser diodes. The absorption cross-section of the Yb^{3+} ion can be calculated by

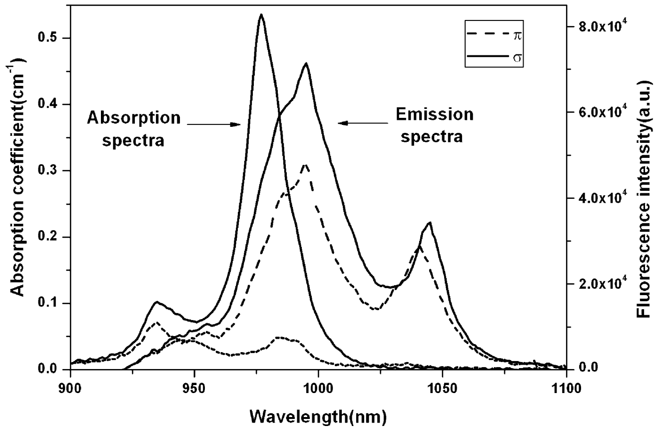

FIGURE 2 The polarized absorption and emission spectra excited by the 980 nm light of Yb^{3+}:GAB at room temperature

$$\sigma_a = \alpha / N_c\,, \tag{1}$$

where α is the absorption coefficient and $\alpha = A/L \log e$, A is the absorbance, and L is the thickness of the polished crystal.

The polarized emission spectra of Yb^{3+}:GAB by excitation with 980 nm at room temperature are also presented in Fig. 2. The σ-polarized emission is stronger than the π-polarized one too. For σ-polarized emission spectrum, two main emission peaks are centered at 995 nm and 1045 nm, respectively. The emission cross-sections can be estimated by the Füchtbauer–Ladenburg equation [3]:

$$\sigma^{FL}_{\pi,\sigma}(\lambda) = \frac{\lambda^5}{8\pi c n^2 \tau_r} \frac{3 I_{\pi,\sigma}(\lambda)}{\int [2 I_\sigma(\lambda) + I_\pi(\lambda)]\, \lambda\, d\lambda}\,, \tag{2}$$

where n is the refractive index of the crystal, and $I_{\pi,\sigma}(\lambda)$ is the π- or σ-polarized emission intensity, and τ_r is the radiative lifetime which is derived from the fluorescence decay curve in the lowest Yb concentrated sample (0.5%) measured at room temperature to be 569 μs as it is shown in Fig. 3.

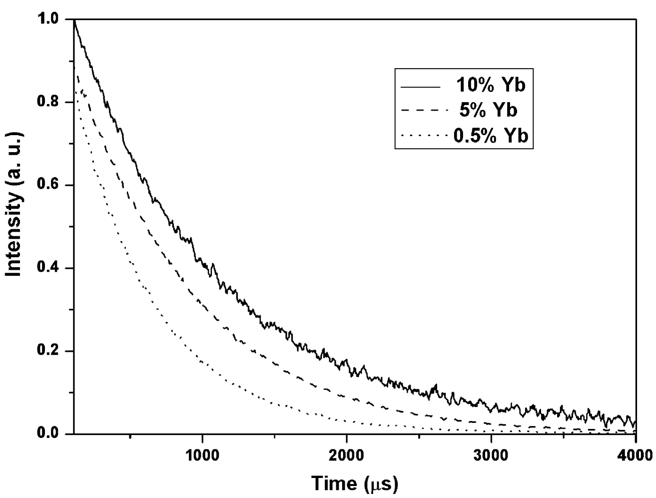

FIGURE 3 The room-temperature fluorescence decay curves of Yb^{3+}:GAB excited at 980 nm

4 Laser performance

4.1 *Laser parameters*

The assessment of Yb^{3+}:GAB crystal involves several parameters influencing laser performance. The first important parameter is β_{min}, which is defined as the minimum inversion fraction of Yb^{3+} ions that must be excited to balance the gain exactly with the ground-state absorption at the laser wavelength λ_{ext}. The value of β_{min} is simply calculated from the absorption and emission cross sections at λ_{ext} by use of the following equation [3]:

$$\beta_{min} = [\sigma_{abs}(\lambda_{ext})] \Big/ [\sigma_{ext}(\lambda_{ext}) + \sigma_{abs}(\lambda_{ext})] \ . \quad (3)$$

The second important parameter is the pump saturation intensity, I_{sat}, that characterizes the pumping dynamics. I_{sat} is a measure of the ease with which the Yb^{3+} population can be bleached to overcome ground-state absorption. A lower I_{sat} value implies a lower flux threshold for laser oscillation. It can be represented as follows [3]:

$$I_{sat} = hc \Big/ \left[\lambda_{pump}\sigma_{abs}(\lambda_{pump})\tau_r\right] \ , \quad (4)$$

where λ_{pump} is the pump wavelength. Since InGaAs diode laser sources are regarded as peak-power-limited devices, a larger pump cross section and a longer emission lifetime lead to a low value of I_{sat} and to an accumulation of a greater population inversion for a peak power.

The minimum absorption pump intensity, I_{min}, is the third important parameter, which is utilized as a figure of merit. This parameter is required for threshold to be reached. It can be calculated by the following expression [3]:

$$I_{min} = \beta_{min} I_{sat} \ . \quad (5)$$

Efficient laser materials doped with Yb^{3+} ions should have a threshold intensity I_{min} as low as possible to obtain the highest extraction cross section. These calculated laser parameters were collected in Table 1.

Another interesting parameter is the gain cross sections, $\sigma_g(\lambda)$, which leads to an estimation of the probable operating laser wavelength and can be obtained using the following formula [8]:

$$\sigma_g(\lambda) = P\sigma_{em}(\lambda) - (1-P)\sigma_{abs}(\lambda) \ , \quad (6)$$

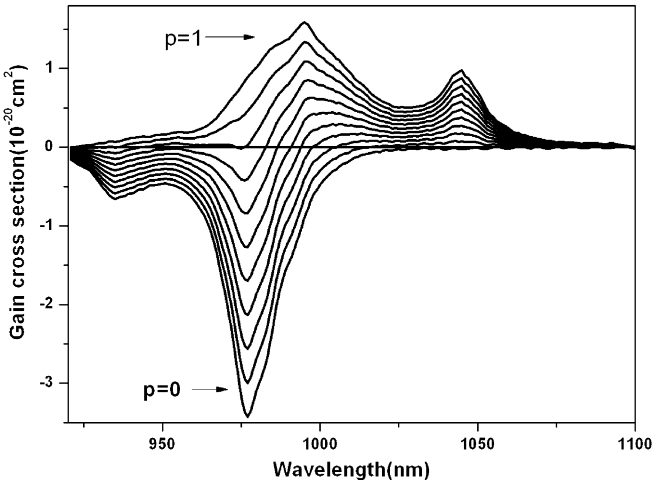

FIGURE 4 The gain cross section in σ-polarization calculated for different values of P for the $^2F_{5/2} \rightarrow {}^2F_{7/2}$ transition of Yb^{3+} in Yb^{3+}:GAB crystal

where P is an inversion population of Yb. For σ-polarization, the gain cross sections σ_g were calculated for several values of population inversion P ($P = 0, 0.1, 0.2, \ldots, 1.0$) and shown in Fig. 4. From these results, we find that the population inversion rate needed to achieve lasing is expected to be only higher than 0.1. For a population inversion level of 0.5, the gain is produced in the 991 ∼ 1098 nm, with the maximum gain cross section of 0.48×10^{-20} cm^2 at the wavelength of 1045 nm. It implies the possible application of Yb^{3+}:GAB as a laser crystal operation at close to 1045 nm.

4.2 *Laser operation*

The 5% doped Yb^{3+}:GAB crystal with a 1.3 mm thickness was used for the laser experiments. The crystal was located inside a 4 cm length plano-concave laser cavity. The input mirror is a plane dichroic mirror coated for high reflection in the 1020–1080 nm range of wavelengths and high transmission at 974 nm pumping wavelength. The concave output coupler has a radius of curvature of 5 cm and a reflectance of 98% near 1040 nm. The Yb^{3+}:GAB laser crystal is mounted in a copper heat sink and located at 5 mm from the plane mirror. The temperature of the copper heat sink is maintained at 15 °C by a flow of water. The pumping beam is provided by a fiber-coupled HLU15F200 laser diode from

Crystal	GAB	GAB*	YAB	YAG	FAP	YCOB	GCOB
λ_{pump} (nm)	977	978	975	942	905	976	902
FWHM (nm)	20	22	20	18	2.4	–	15
$\sigma_{abs}(\lambda_{pump})(10^{-20}$ cm$^2)$	3.43	2.5	3.4	0.8	10	0.94	0.41
λ_{ext} (nm)	1045	1040	1040	1031	1043	1030	1032
$\sigma_{ext}(\lambda_{ext})$ $(10^{-20}$ cm$^2)$	0.98	0.7	0.8	2.0	5.9	0.55	0.55
τ (ms)	0.569	0.298	0.68	1.08	1.08	2.65	2.6
β_{min}	0.022	–	0.043	0.055	0.046	0.058	0.06
I_{sat} (kW/cm^2)	10.4	–	8.8	28	2.6	8.2	25.5
I_{min} (kW/cm^2)	0.23	–	0.38	1.54	0.132	0.48	1.54
Ref.	This work	[14]	[6]	[3]	[4]	[7]	[8]

* Yb^{3+} ion doped concentration is 12.5 at. %

TABLE 1 Spectroscopic and laser parameters of Yb^{3+}:GAB and other Yb^{3+}-doped crystals

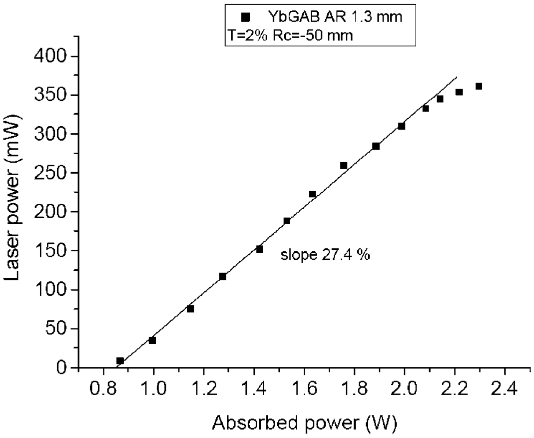

FIGURE 5 The output power of the Yb^{3+}:GAB laser at 1043 nm as a function of the absorbed pump power

LIMO (Germany). The pump is focused into the laser crystal by two 60 mm focal length doublets. The diameter of the pumping beam in the laser crystal is 230 μm.

The wavelength of the laser emission was measured to be 1043 nm. The output power versus the absorbed pump power is shown in Fig. 5. The obtained slope efficiency was 27.4%.

Let us notice that the pumping of the crystal is accompanied by a weak green light located at the focal point. It is attributed to up-conversion towards unwanted traces of Er^{3+} emitting near 550 nm. But this phenomenon is weak and we do not believe that it influences the lasing efficiency.

5 Results and discussion

From the polarized absorption and emission spectra shown in Fig. 2, it can be found that the Yb^{3+}:GAB crystal shows strong polarization dependence. In both the absorption and emission spectra, the intensities of the σ-polarization are stronger than those of the π-polarization. Thus, the σ-polarized absorption and emission spectra were used to calculate the spectroscopic and parameters relevant for laser operation. For σ-polarization, the strongest emission peak is located at 995 nm, but it overlaps the edge of the strongest absorption peak at the wavelength of 977 nm, which leads to a large reabsorption loss and difficulty in lasing this channel [3, 6]. Thus, this wavelength cannot be used for practical laser output. The second strongest peak at 1045 nm is thus usually used for laser output.

From Fig. 3, the fluorescence lifetimes of the 0.5%, 5% and 10% Yb doped concentration sample are derived to be 569, 800 and 993 μs, respectively. They are all single exponential. And we can see that the fluorescence lifetimes increase when the Yb ions concentration increases from the lowest value 0.5% up to 10%. This can be explained by the well-known phenomena of radiation trapping due to the large overlap between the emission and absorption spectra of the Yb ion [13]. However, adding in Table 1 the 298 μs lifetime data obtained in [14] for a heavily doped sample (12.5% Yb), we can see that further increases of concentration lead to a short lifetime, may be due to its special measurement techniques, that the crystal powder was immersed inside a index matching liquid to eliminate radiation trapping and total internal reflection, but then the measured lifetime would be varied with the preparation of the powder and the surroundings, such as the size of the particle, the density of the powder and the refractive index of the index matching liquid [15–17].

According to our work, the spectroscopic properties of Yb^{3+}:GAB are more similar than the ones of Yb^{3+}:YAB. However in Table 1 we can see that the emission cross-section in GAB is slightly higher than in YAB. Furthermore, the laser parameters β_{min}, and I_{min} are lower than those of Yb^{3+}:YAB, implying that Yb^{3+}:GAB may have better laser properties. On comparing laser operation, an output power of 4.3 W at 1040 nm, with a slope efficiency as high as 48% and a pump power threshold of $\sim$ 2 W has been demonstrated in Yb^{3+}:YAB [12]. In the present work, about 0.4 W laser output power at 1043 nm with a 27.4% slope efficiency and a pump power threshold of $\sim$ 0.8 W was obtained in Yb^{3+}:GAB crystal. But we have to notice that the Yb^{3+}:GAB crystal used was not optimised: it has only 51% pump absorption and its anti-reflection coating was not effective; the one-pass transmission of the sample was only 98% at 1100 nm. Moreover, the laser diode used for pumping emitted at 974 nm and not at 977 nm. The 2% output coupling was not optimized because no systematic attempts with different mirrors were performed at this early stage of our study. Thus, we can think that much better performances will be obtained in a further work with optimised conditions.

In summary, the spectroscopic and laser investigations show that Yb^{3+}:GAB crystal satisfies the conditions for laser operation. The Yb:GAB crystal used in this work is not oriented in a direction of phase matching for frequency doubling. This is why the interesting topic of the nonlinearity of the crystal is not investigated in this paper. But a further work with oriented crystals is in progress because we think that this material has a high potential to be an efficient self-frequency-doubling crystal for green and possibly yellow lasers.

ACKNOWLEDGEMENTS This work was supported by the Nature Science Foundation of Fujian province (No.E0410028), the Innovative Project of Chinese Academy of Sciences (KJCX2-SW-h05), the Frontier & Interdisciplinary project of FJIRSM, CAS and the CNRS network "Cristaux Massifs et Dispositifs pour l'Optique" (CMDO).

REFERENCES

1 E.C. Honea, R.J. Beach, S.C. Mitchell, J.A. Skidmore, M.A. Emanuel, S.B. Sutton, S.A. Payne, P.V. Avizonis, R.S. Monroe, D.G. Harris, Opt. Lett. **25**, 805 (2000)
2 P. Lacovara, H.K. Choi, C.A. Wang, R.L. Aggarwal, T.Y. Fan, Opt. Lett. **16**, 1089 (1991)
3 L.D. Deloach, S.A. Payne, L.L. Chase, L.K. Smith, W.L. Kway, W.F. Krupke, IEEE J. Quantum Electron. **QE-29**, 1179 (1993)
4 S.A. Payne, L.D. DeLoach, L.K. Smith, W.L. Kway, J.B. Tassano, W.F. Krupke, J. Appl. Phys. **76**, 497 (1994)
5 L.A.W. Gloster, P. Cormont, A.M. Cox, T.A. King, B.H.T. Chai, Opt. Commun. **146**, 177 (1998)
6 P. Wang, J.M. Dawes, P. Dekker, D.S. Knowles, J.A. Piper, B. Lu, J. Opt. Soc. Am. B **16**, 63 (1999)
7 H. Jiang, J. Wang, H. Zhang, X. Hu, P. Burns, J.A. Piper, Chem. Phys. Lett. **361**, 499 (2002)
8 F. Mougel, K. Dardenne, G. Aka, A. Kahu-harari, D. Vivien, J. Opt. Soc. Am. B **16**, 164 (1999)
9 A. Brenier, C. Tu, Z. Zhu, J. Li, Y. Wang, Z. You, B. Wu, Appl. Phys. Lett. **84**, 16 (2004)

10 A. Brenier, C. Tu, Z. Zhu, J. Li, B. Wu, J. Appl. Phys. **97**, 013 503 (2005)
11 A. Brenier, C. Tu, Z. Zhu, B. Wu, Appl. Phys. Lett. **84**, 2034 (2004)
12 P. Dekker, J.M. Dawes, J.A. Piper, Y. Liu, J. Wang, Opt. Commun. **195**, 431 (2001)
13 D.S. Sumida, T.Y. Fan, Opt. Lett. **19**, 1343 (1994)
14 J. Liao, Y. Lin, Y. Chen, Z. Luo, Y. Huang, J. Cryst. Growth **269**, 484 (2004)
15 F.D. Patel, E.C. Honea, J. Speth, S.A. Payne, R. Hutcheson, R. Equall, IEEE J. Quantum Electron. **QE-37**, 135 (2001)
16 H.P. Christensen, D.R. Gabbe, H.P. Jenssen, Phys. Rev. B **25**, 1467 (1982)
17 M.C. Pujol, M.A. Bursukova, F. Guell, X. Mateos, R. Sole, J. Gavalda, M. Aguilo, J. Massons, F. Diaz, P. Klopp, U. Griebner, V. Petrov, Phys. Rev. B **65**, 165 122 (2002)